SCIENCE CHINA
Chemistry

• ARTICLES •

June 2013 Vol.56 No.6: 806–812
doi: 10.1007/s11426-012-4819-z

Mercuric ions induced aggregation of gold nanoparticles as investigated by localized surface plasmon resonance light scattering and dynamic light scattering techniques

WANG Wei[1], LIU Chun[2], LING Jian[2] & HUANG ChengZhi[1,2*]

[1]*College of Pharmaceutical Sciences, Southwest University, Chongqing 400715, China*
[2]*Education Ministry Key Laboratory on Luminescence and Real-Time Analysis, College of Chemistry and Chemical Engineering, Southwest University, Chongqing 400715, China*

Received September 23, 2012; accepted November 14, 2012; published online January 6, 2013

With the development of nanosciences, both localized surface plasmon resonance light scattering (LSPR-LS) and dynamic light scattering (DLS) techniques have been widely used for quantitative purposes with high sensitivity. In this contribution, we make a comparison of the two light scattering techniques by employing gold nanoparticles (AuNPs) aggregation induced by mercuric ions. It was found that citrate-stabilized AuNPs got aggregated in aqueous medium in the presence of mercuric ions through a chelation process, resulting in greatly enhanced LSPR-LS signals and increased hydrodynamic diameter. The enhanced LSPR-LS intensity (ΔI) is proportional to the concentration of mercuric ions in the range of 0.4–2.5 μM following the linear regression equation of $\Delta I = -84.7+516.4c$, with the correlation coefficient of 0.983 ($n = 6$) and the limit of determination (3σ) about 0.10 μM. On the other hand, the increased hydrodynamic diameter can be identified by the DLS signals only with a concentration of Hg^{2+} in the range of 1.0–2.5 μM, and a linear relationship between the average hydrodynamic diameters of the resulted aggregates and the concentration of Hg^{2+} can be expressed as $d = -6.16 + 45.9c$ with the correlation coefficient of 0.994. In such case, LSPR-LS signals were further applied to the selective determination of mercuric ions in lake water samples with high sensitivity and simple operation.

gold nanoparticles (AuNPs), localized surface plasmon resonance light scattering (LSPR-LS), dynamic light scattering (DLS), mercury, aggregation

1 Introduction

Localized surface plasmon resonance light scattering (LSPR-LS) and dynamic light scattering (DLS) are two analytical techniques, and both of which are based on the size-dependent light scattering properties of particles. LSPR-LS technique depends upon the measurements of the light scattering of metal nanoparticles resulting from the so-called localized surface plasmon resonance (LSPR), the radiation of collective oscillation of the surface conduction electron when excited by electromagnetic radiation [1]. Starting ten years ago [2], the LSPR-LS technique has been extensively applied in analytical detections such as those of DNA hybridization [3], amino acids [4], toxic heavy metals [5] and also in immunoassay [6]. Different from LSPR-LS, DLS is a common used technique for estimating the sizes and distributions of variety of particles in high polymer and pharmaceutical sciences [7], crystallization studies [8] and the biophysical characterizations of the influence of salt concentration [9], pH [10], and protein behavior [11], and has recently been used in quantitative analysis in combination with gold nanoparticles (AuNPs) [12–14]. It should be noted that the parameters of both DLS intensity and diameter size have been employed for quantitative purposes, but the later one is much more popular [12,14].

*Corresponding author (email: chengzhi@swu.edu.cn)

Although both LSPR-LS and DLS can be applied for quantitative purposes, they are intrinsically different in principle. First, LSPR-LS signals, which contain not only pure Rayleigh scattering, but also other light scattering signals including Mie, Tyndall, and Brillouin light scattering, have been widely applied in the designation of bioassemblies and aggregation process, while DLS is known as photon correlation spectroscopy or quasi-elastic light scattering based on the monitoring of the time-varying fluctuations in scattered light intensities caused by the Brownian motion [7]. Second, the LSPR-LS occurs from the differences in polarizability between the aggregates of metal nanoparticles and the solvent, and when the incident electromagnetic wave induces an oscillating dipole in the assembly, the light radiates in all directions [15]. However, DLS depends on the Brownian motion of spherical particles which causes a Doppler shift of incident laser light, and then the size of the particles can be calculated using the Stokes-Einstein equation on the basis of the measurements of the diffusion coefficient of particles [16]. As a matter of fact, LSPR-LS signals demonstrate the whole optical properties of the suspension of metal nanoparticles, while DLS measurements detect the average hydrodynamic diameter of the whole nanoparticle or aggregate population.

AuNPs are well known for their large plasmon resonance absorption and scattering cross section in their LSPR wavelength regions [2], and their LSPR properties can be facilely tuned through the change of their size, shape and distance [17]. The aggregation or de-aggregation of AuNPs often leads to the changes of optical properties, such as the LSPR-LS and DLS. Consequently, both LSPR-LS and DLS techniques have been extensively applied for AuNPs agglutination-based biomolecular detection or immunoarray [4,12]. Moreover, the aggregation of AuNPs enhances the LSPR-LS response, providing several advantages with respects to simple preparation, easy readout, good stability and high sensitivity.

Mercury is known as a highly toxic metal element and a widespread pollutant in environment. Mercury toxicosis can damage the nervous system, genetic and enzyme systems, immune system and many organs, threatening the health of human being and wildlife severely [18]. Owing to the bioaccumulation of mercury from soil, water and atmosphere and biomagnifications by ingesting mercury-containing organisms, people readily absorb mercury unconsciously. Up to now, most traditional techniques including colorimetry [19], fluorescence spectroscopy [20], electrochemistry [21], and inductively coupled plasma mass spectrometry (ICP-MS) [22], have been widely applied in monitoring mercury levels in aqueous environments. Among these methods, AuNPs have also been employed in detecting mercury content based on the size and distance-dependent LSPR absorption properties. For example, Chang [23] and Liu [24] have proposed the novel colorimetric assays on the basis of T-Hg-T coordination and AuNPs aggregation. Through the nanomaterial surface energy transfer from the donor of organic dye Rhodamine B to the receptor of AuNPs surface [25], some fluorescent sensors for mercury ions have been developed. These methods, although having highly improved selectivity and sensitivity, still suffer from the limitations with respect to operation complex, time-consuming or the use of expensive instruments. Hence, facile, rapid and visual detections for mercuric ions are still desirable.

In this contribution, we select the binding between mercuric ion and citrate-stabilized AuNPs as a model system and make a comparison of the two light scattering techniques, LSPR-LS and DLS (Figure 1), in terms of analytical purposes, and then propose a method for detecting mercury in water environments. The binding of mercury ion to the citrate causes the aggregation of AuNPs, and the subsequent average hydrodynamic diameter and light scattering signals get increased, which correlates to the mercury concentration as measured by LSPR-LS and DLS, respectively. The further investigations show that the LSPR-LS technique can be employed in a one-step highly sensitive method for mercury ion detection in water environments.

2 Experimental

2.1 Materials

Mercury chloride ($HgCl_2$) and hydrogen tetrachloroaurate tetrahydrate ($HAuCl_4{\cdot}4H_2O$) were commercially obtained from Chuandong Chemical Group Co., Ltd. (Chongqing, China) and Sinopharm Group Chemical Regent Co., Ltd. (Shanghai, China), respectively. All other reagents in this experiment were analytical reagent grade and used without further purification.

AuNPs were prepared by citrate reduction of $HAuCl_4$ according to literature [26] with slight modification. Briefly, 1.0 mL of 5.0% trisodium citrate solution was rapidly added into 49 mL boiling solution containing 1 mL 1% $HAuCl_4$ under vigorous stirring. The solution was boiled for another

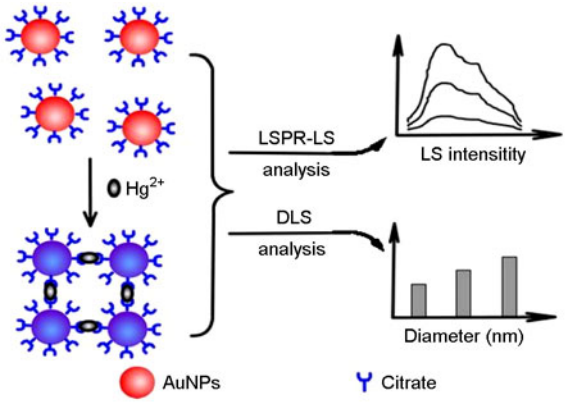

Figure 1 Schematic illustration of aggregation of metalnanopaticles investigated by localized surface plasmon resonance light scattering and dynamic light scattering techniques.

5 min until its color changed from blue into red. Then the solution was cooled down to room temperature with continuous stirring. The concentration of AuNPs was estimated to be ca. 22 nM, which was calculated from its absorbance at 520 nm according to Beer's law by using the extinction coefficient of ca. 10^8 M^{-1} cm^{-1} for 13 nm AuNPs [26]. All glassware prior to use in the preparation procedures were thoroughly cleaned with aqua fortis and water. Milli-Q purified water (18.2 MΩ, LD-50G-E Lidi Ultra Pure Waters System, Chongqing, China) was used throughout.

2.2 Apparatus

Localized surface plasmon resonance light scattering (LSPR-LS) spectrum and intensity were measured with an F-2500 fluorescence spectrophotometer (Hitachi, Tokyo, Japan). The hydrodynamic diameters of particles were determined with a N5 Submicron Particle Size Analyzer (Beckman, California, USA). Direct mercury measurements were performed on DMA-80 Direct Mercury Analyzer (Milestone, Italy). The UV absorption spectra were obtained with a U-3010 spectrophotometer (Hitachi, Tokyo, Japan). An S-4800 scanning electron microscopy (Hitachi, Tokyo, Japan) was used to measure the size and shape of AuNPs. A pHS-3C digital pH meter (Leici, Shanghai, China) was used to detect the pH values. A QL-901 vortex mixer (Linqibeier, Haimen, China) was employed for solution blending.

2.3 Procedures

Into a 1.5 mL centrifugal tube, 13 nM AuNPs, Tris-HCl buffer (15 mM, pH 7.4), and $HgCl_2$ (0–2.5 μM) solution were added. The mixture was then diluted to 500 μL with water and blended thoroughly with a vortex mixer. In this paper, the final concentrations of the species are provided. It should be noted that the order of the addition of the reagents is of great concern for the light scattering measurement, which might be ascribed to the irreversible reaction. After incubation at room temperature for 10 min, the LSPR-LS spectra were measured against the reagent blank solution treated in the same way only without Hg^{2+}.

LSPR-LS spectra were obtained by scanning simultaneously the excitation and emission monochromators of the F-2500 fluorescence spectrophotometer synchronously with the same excitation and emission wavelengths (namely, $\Delta\lambda$ = 0 nm) in the range from 220 to 700 nm, and the LSPR-LS intensities were measured at the wavelength of 344 nm. The slit width and PMT voltage of the measurements were kept throughout at 5 nm and 400 V, respectively.

3 Results and discussion

3.1 Aggregation of citrated-AuNPs induced by mercuric ions

The citrated-AuNPs prepared according to literature were surrounded by carboxylate, which makes the nanoparticles in dispersed state owing to the electrostatic repulsion interaction and renders the solution red. In the presence of aqueous mercury, aggregation of AuNPs occurred because of the intense affinity of simple carboxylic acid for mercuric ions [27]. To verify the formation of aggregates, we conducted scanning electron microscopy imaging analysis to investigate the morphology of AuNPs before and after dealing with Hg^{2+}. The SEM images are displayed in Figure 2, it is clear that the AuNPs are well monodispersed with the size about 13 nm (Figure 2(A)), and the degree of aggregation of the AuNPs enhanced obviously with the increasing concentration of Hg^{2+} (Figure 2(B) and (C)).

Meanwhile, owing to the concomitant strong plasmon resonance absorption (PRA) band shift or broadening, this aggregation phenomenon also can be easily monitored by UV-vis absorption spectroscopy or visual observation. Aqueous suspensions of the 13 nm gold nanoparticles display an intense PRA band centering around 520 nm (Figure 3(a)) that renders the suspensions red. However, upon the addition of Hg^{2+}, the peak of 520 nm gets decreased gradually, and a new peak at 640 nm comes into being (Figure 3, (b–f)). This red shift is caused by electric dipole-dipole interaction and coupling between the plasmons of neighboring particles in the formed aggregates [4]. Corresponding to the red shift of the PRA band, a clear red-to-blue color response can be observed within 10 min.

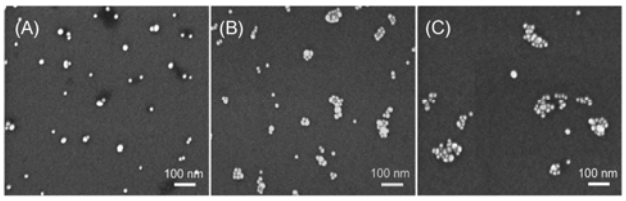

Figure 2 The SEM images of AuNPs in the absence (A) and presence of (B) 1.5 μM Hg^{2+} and (C) 2.5 μM Hg^{2+} in 15 mM Tris-HCl buffer of pH 7.4.

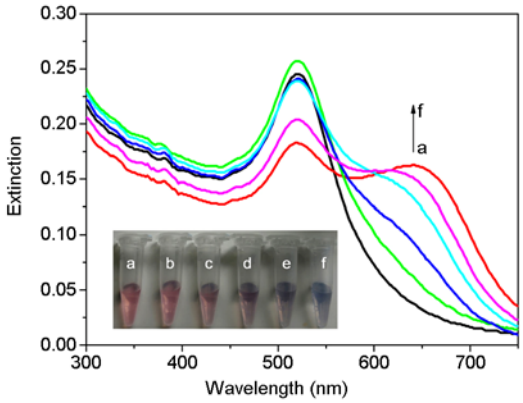

Figure 3 UV-vis absorption spectra of AuNPs in the Tris-HCl buffer (15 mM, pH 7.4) upon addition of different concentrations of Hg^{2+}. $c_{Hg(II)}$ (μM): (a) 0, (b) 0.5, (c) 1.0, (d) 1.5, (e) 2.0, (f) 2.5. The incubation time was 10 min.

3.2 LSPR features of AuNPs aggregates

Besides the shift of PRA band, the aggregation of AuNPs also causes the enhancement of LSPR-LS response, which can be monitored with a common spectrofluorometer as described in our previous reports [28, 29], and increases the average size as expressed by hydrodynamic diameter, which can be detected by DLS technique. Figure 4 shows the LSPR-LS spectra of AuNPs upon addition of increasing concentrations of Hg^{2+}. As it can be seen, the light scattering signals of AuNPs in the absence of mercuric ion are weak in whole scanning wavelength region of 220–700 nm (Figure 4(a)), and the signals get enhanced with the addition of mercuric ions. The enhanced light scattering increased gradually in good linearity over the range of 0.4–2.5 μM, and the linear regression equation is $\Delta I = -84.7+516.4c$ (c, μM) with the correlation coefficient 0.983, The limit of determination (3σ) is 0.10 μM (Figure 4, b–g and inset), revealing that the intensity of light scattering has concentration-dependent relationship with mercuric ions and can be applied for analytical purposes.

According to the literature [15], the LSPR-LS intensity is correlative with the formation of the aggregate and its particle dimension in solution. In other words, the aggregation of AuNPs and the interparticle coupling can result in great enhancement of light scattering. The relationship between light scattering intensity and particle radius can be expressed by the following Rayleigh equation [2]:

$$I = \frac{16\pi^4 a^6 n_{\text{med}}^4 I_0}{r^2 \lambda_0^4} \left| \frac{m^2 - 1}{m^2 + 2} \right|^2 \sin^2(\alpha) \qquad (1)$$

wherein I_0 is the intensity of incident monochromatic light, λ_0 the wavelength of the incident beam, a the radius of spherical particle, n_{med} the refractive index of the medium surrounding the particle, α the angle between the detection direction r and the direction of polarization of the incident beam, and m is the relative refractive index of the bulk particle material. Thus, the aggregation of AuNPs induced by the mercuric ion leads to the size increase of scatters, resulting in enhanced light scattering signals. Because the intensity of scattered light varies with the sixth power of the particle radius at a given wavelength [2], slight alteration of particle radius can induce great change of scattered light intensity.

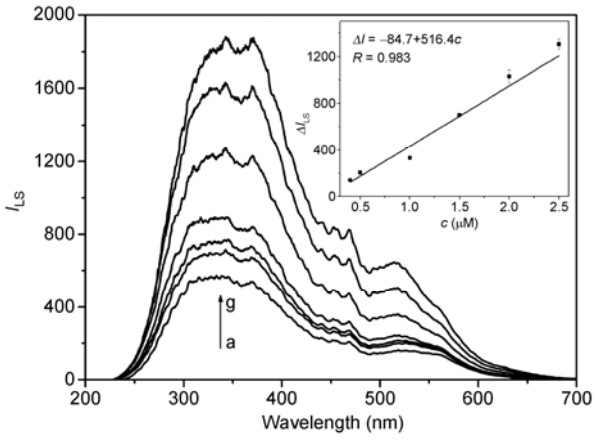

Figure 4 LSPR-LS spectra of AuNPs (13 nM) in the Tris-HCl buffer (15 mM, pH 7.4) by increasing concentrations of Hg^{2+}. $c_{Hg(II)}$ (μM): (a) 0, (b) 0.4, (c) 0.5, (d) 1.0, (e) 1.5, (f) 2.0, (g) 2.5. Inset: The calibration curve of the mercuric ions concentration in the range of 0.4–2.5 μM versus the intensity of the light scattering at 344 nm. The linear regression equation is $\Delta I = -84.7+516.4c$ and the corresponding correlation coefficient is 0.983 (n = 6) and the limit of determination (3σ) is 0.10 μM.

3.3 Dynamic light scattering detection of AuNPs aggregates

On the other hand, the aggregation caused by the binding of Hg^{2+} with citrate-stabilized gold nanoparticles increases the average diameter of the whole nanoparticle population which can be monitored by DLS analysis. Moreover, the increase of average diameter is correlated quantitatively to the Hg^{2+} concentration. Figure 5 shows, the DLS signals which were detected with the incident laser wavelength at 632.8 nm, following the Stokes-Einstein equation on the basis of the measurements of the diffusion coefficient of particles, reveal that the AuNPs of the size about 13 nm has mean hydrodynamic diameter of 42.2 nm, and it can get increased upon increasing concentration of Hg^{2+} primarily because of the increased aggregation of AuNPs. It can be seen that the change of particle size was too slight to be detected by DLS in low concentration of Hg^{2+}. When the concentration of mercuric ions was in the range of 1.0–2.5 μM, we then could observe the linear relationships between the average hydrodynamic diameters of the resulted aggregates and the concentration of Hg^{2+}, which could be expressed as $d = -6.16 + 45.9c$ with corresponding correlation coefficient of 0.994.

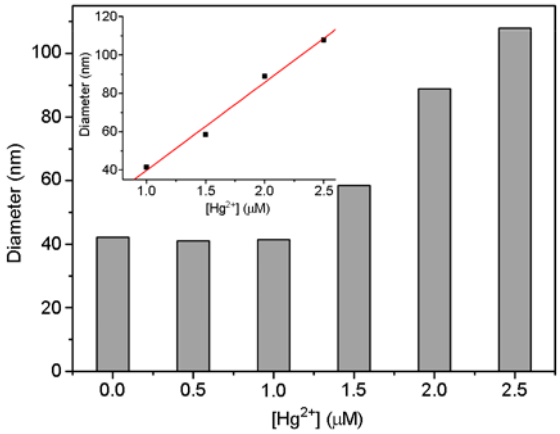

Figure 5 The average diameters of AuNPs as detected from DLS measurement and plotted against the mercuric ions concentration. AuNPs 13 nM, Tris-HCl buffer 15 mM, pH 7.4. Tested angle 90°, temperature 24 °C, incident laser wavelength: 632.8 nm, laser power 25 mW. The mean hydrodynamic diameter of AuNPs without mercuric ions is 42.2 nm.

The DLS technique depends on time-varying fluctuations in scattered light intensities caused by Brownian motion. Then, the diffusion constant of particles can be measured and the sizes of the particles are calculated using the Stokes-Einstein relation [30]:

$$D = \frac{k_B T}{6\pi\eta R} \quad (2)$$

In this equation, D denotes the translational diffusion coefficient, k_B is Boltzmann's constant, T is the absolute temperature, η is the viscosity of the suspending medium and R is particle radius. Particles in different sizes are undergoing different Brownian motion rate, and thus have different light scattering fluctuation rate. So, AuNPs aggregates and dispersed AuNPs can be distinguished using DLS technique.

Although being an alternative choice to monitor particle agglutination, DLS technique suffers from the sensitivity contrast to LSPR-LS assay. As above mentioned, an obvious increase in LSPR-LS intensity is observed with the addition of as low as 0.4 μM Hg^{2+} (Figure 4), a concentration low to yield a visible color change (Figure 3 inset). However, the hydrodynamic diameter of AuNPs can not be distinguished by DLS technique when the concentration of Hg^{2+} is below 1.0 μM. From the working principle, we can conclude that, to the same increase of the particle size, the LSPR-LS technique is more sensitive than the DLS technique because the former is based on the theory that the intensity of light scattering is proportional to sixth power of the particle radius and the latter detects the diffusion coefficient which is only in inverse proportion to the particle size according to the Stokes-Einstein relation [2, 30].

3.4 Optimal condition for the AuNPs aggregation induced by mercuric ions

Above results showed that LSPR-LS assay can monitor the increase of the aggregation with the addition of aqueous mercuric ions, thus it can be applied further in detecting Hg^{2+} in water sample. By keeping conditions fixed, we examined the influence of pH-value that was controlled by 15 mM Tris-HCl buffer with different concentration ratios of Tris to HCl in the pH range of 7.1–8.1 (Figure 6). In this pH range, light scattering signals of AuNPs almost kept constant. With the addition of mercuric ions, however, the light scattering signals highly enhanced and formed a platform in the pH range of pH 7.2–7.6.

Changes in the light scattering intensity caused by other metal ions and haloid ions, including Zn^{2+}, Ba^{2+}, Co^{2+}, Pb^{2+}, Cu^{2+}, Cd^{2+}, Mg^{2+}, Ni^{2+}, Mn^{2+}, Ca^{2+}, K^+, Na^+, Br^- and I^- were also measured. The LSPR-LS responses of AuNPs, recorded 10 min later after the addition of different amount of each of these ions, are displayed in Figure 7. Only Mg^{2+}, Cu^{2+} and I^- can result in slight LSPR-LS intensity changes when they are present in 100-folds higher than Hg^{2+}, while

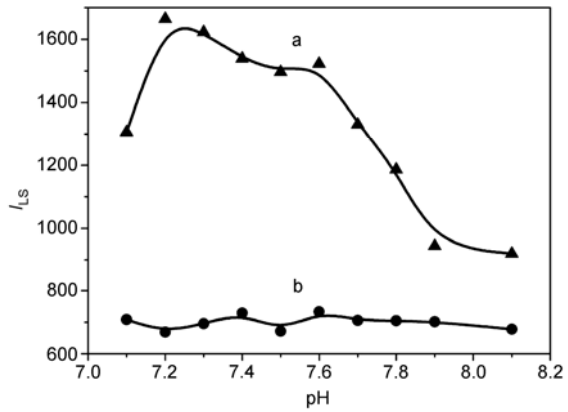

Figure 6 Effect of pH on the LSPR-LS response of AuNPs in the absence and the presence of Hg^{2+}. (a) 13 nM AuNPs +1.5 μM Hg^{2+} and (b) 13 nM AuNPs in buffer. The pH values of the solutions were controlled by 15 mM Tris-HCl buffer with different concentration ratios of Tris to HCl in the pH range of 7.1–8.1. The incubation time for AuNPs-Hg^{2+} is 10 min. λ = 344 nm.

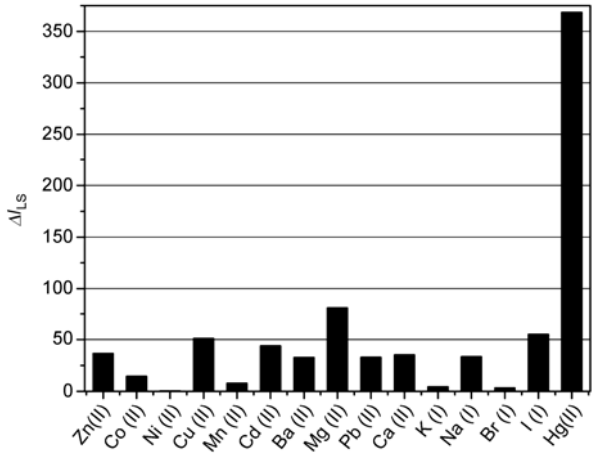

Figure 7 LSPR-LS response of AuNPs upon the addition of various ions. $c_{Hg(II)}$: 1.5 μM. All the concentrations of other ions were 150 μM except that of Zn^{2+} being 15 μM and that of Na^+ being 1.5 mM. 15 mM Tris-HCl buffer of pH 7.4 was used. λ = 344 nm.

other ions do not cause any significant changes under identical conditions. This experimental result coincides with the principle that the stability constant of Hg^{2+} is higher than that of other metal ions [27] for carboxylate. In other words, the affinity of carboxylate for Hg^{2+} is more intense than for other metal ions, which is why this assay showed a good selectivity of Hg^{2+}.

3.5 Applications of the AuNPs aggregation induced by mercuric ions

The calibration curve for determination of mercury ions is constructed under the optimum condition and the LSPR-LS intensity enhanced linearly over the range 0.4–2.5 μM with the corresponding limits of determination (3σ) of 0.1 μM.

Thus, the goal of 2 ppb (10 nM) defined as the maximum contamination level for drinking water by the US Environmental Protection Agency (EPA) can be theoretically achieved by pre-concentrating the water solution.

According to the calibration curve, three artificial samples of Hg^{2+} with some metal ions or haloid anions are simultaneously determined under the same conditions. The determination results are listed in Table 1. As Table 1 presents, the recoveries covered from 92.0 to 105.0% with the RSD below 5.4%. Namely, this approach can be used to detect practical samples. By applying a standard addition method, we further detected water samples obtained from Chongde pond on the campus of our university. The samples collected were filtered through a 0.22 μm Millipore syringe for three times to remove the solid impurity. Table 2 displays the detection results of lake water samples using LSPR-LS method and direct mercury analyzer. The results of LSPR-LS method were in agreement with the results determined by direct mercury analyzer, suggesting that this method is reliable.

4 Conclusions

In this contribution, we made a comparison of two light scattering techniques, LSPR-LS and DLS, in terms of analytical purposes by detecting the AuNPs aggregation induced by citrate coordination of Hg^{2+}, and found that both of them are powerful tools to investigate the aggregation of metal nanoparticles, and that LSPR-LS method is much more sensitive than DLS method. By employing LSPR-LS assay, we also developed a facile and rapid detection of Hg^{2+} with good sensitivity (0.10 μM) and selectivity. Furthermore, this approach demonstrated feasibility of detection of Hg^{2+} over a number of environmentally relevant ions in water samples. According to these results, we can draw out that LSPR-LS can be a sensitive and cheap tool for characterization of gold nanoparticles and their aggregates.

Table 1 Determination results for artificial samples[a)]

Samples	Hg^{2+} (μM)	Main additives	Mean found (μM)	Recovery (%)	RSD (%, n = 3)
1	2.00	Ba^{2+}, Cu^{2+}, Pb^{2+}, Cd^{2+}	1.93–2.10	96.5–105.0	4.3
2	1.50	Ca^{2+}, Mg^{2+}, Mn^{2+}, Zn^{2+}	1.38–1.53	92.0–102.0	5.4
3	2.00	Cl^{-}, Br^{-}, I^{-}	1.93–2.00	96.5–100.0	1.8

a) The concentration of AuNPs, 13 nM; 15 mM Tris-HCl buffer pH 7.4. All other ions are 10.0 μM.

Table 2 Determination of mercuric ions in water samples using LSPR-LS method and direct mercury analyzer

Samples	Added (μM)	LSPR-LS method Mean [a)] ±SD (μM)	Direct mercury analyzer found (μM)
Lake water 1	1.2	1.66±0.08	1.69
Lake water 2	1.2	1.68±0.06	1.72

a) Mean of three determinations. Concentration: AuNPs, 13 nM; Tris-HCl buffer, 15 mM, pH 7.4.

This work was supported by the National Natural Science Foundation of China (21035005).

1 Willets KA, Duyne RPV. Localized surface plasmon resonance spectroscopy and sensing. *Annu Rev Phys Chem*, 2007, 58: 267–297
2 Yguerabide J, Yguerabide EE. Light-scattering submicroscopic particles as highly fluorescent analogs and their use as tracer labels in clinical and biological applications I. Theory. *Anal Biochem*, 1998, 262: 137–156
3 Du BA, Li ZP, Liu CH. One-step homogeneous detection of DNA hybridization with gold nanoparticle probes by using a linear light-scattering technique. *Angew Chem Int Ed*, 2006, 45: 8022–8025
4 Li ZP, Duan XR, Liu CH, Du BA. Selective determination of cysteine by resonance light scattering technique based on self-assembly of gold nanoparticles. *Anal Biochem*, 2006, 351: 18–25
5 Fan Y, Long YF, Li YF. A sensitive resonance light scattering spectrometry of trace Hg^{2+} with sulfur ion modified gold nanoparticles. *Anal Chim Acta*, 2009, 653: 207–211
6 Du BA, Li ZP, Cheng YQ. Homogeneous immunoassay based on aggregation of antibody-functionalized gold nanoparticles coupled with light scattering detection. *Talanta*, 2008, 75: 959–964
7 Bloomfield VA. Static and dynamic light scattering from aggregating particles. *Biopolymers*, 2000, 54: 168–172
8 Kadima W, McPherson A, Dunn MF, Jurnak FA. Characterization of precrystallization aggregation of canavalin by dynamic light scattering. *Biophys J*, 1990, 57: 125–132
9 Lee WI, Schurr JM. Dynamic light scattering studies of poly-L-lysine HBr in the presence of added salt. *Biopolymers*, 2004, 13: 903–908
10 Moradian-Oldak J, Leung W, Fincham AG. Temperature and pH-dependent supramolecular self-assembly of amelogenin molecules: A dynamic light-scattering analysis. *J Struct Biol*, 1998, 122: 320–327
11 Gallagher WH, Woodward CK. The concentration dependence of the diffusion coefficient for bovine pancreatic trypsin inhibitor: A dynamic light scattering study of a small protein. *Biopolymers*, 2004, 28: 2001–2024
12 Jans H, Liu X, Austin L, Maes G, Huo Q. Dynamic light scattering as a powerful tool for gold nanoparticle bioconjugation and biomolecular binding studies. *Anal Chem*, 2009, 81: 9425–9432
13 Kalluri JR, Arbneshi T, Afrin Khan S, Neely A, Candice P, Varisli B, Washington M, McAfee S, Robinson B, Banerjee S, Singh AK, Senapati D, Ray PC. Use of gold nanoparticles in a simple colorimetric and ultrasensitive dynamic light scattering assay: Selective detection of arsenic in groundwater. *Angew Chem Int Ed*, 2009, 121: 9848–9851
14 Dai Q, Liu X, Coutts J, Austin L, Huo Q, A one-step highly sensitive

method for DNA detection using dynamic light scattering. *J Am Chem Soc*, 2008, 130: 8138–8139
15 Pasternack RF, Collings PJ, Resonance light scattering: A new technique for studying chromophore aggregation. *Science*, 1995, 269: 935–939
16 Liu X, Dai Q, Austin L, Coutts J, Knowles G, Zou J, Chen H, Huo Q. A one-step homogeneous immunoassay for cancer biomarker detection using gold nanoparticle probes coupled with dynamic light scattering. *J Am Chem Soc*, 2008, 130: 2780–2782
17 Daniel MC, Astruc D. Gold nanoparticles: Assembly, supramolecular chemistry, quantum-size-related properties, and applications toward biology, catalysis, and nanotechnology. *Chem Rev*, 2004, 104: 293–346
18 Langford N, Ferner R. Toxicity of mercury. *J Hum Hypertens*, 1999, 13: 651–656
19 Li L, Li BX, Qi YY, Jin Y. Label-free aptamer-based colorimetric detection of mercury ions in aqueous media using unmodified gold nanoparticles as colorimetric probe. *Anal Bioanal Chem*, 2009, 393: 2051–2057
20 Xia YS, Zhu CQ. Use of surface-modified CdTe quantum dots as fluorescent probes in sensing mercury(II). *Talanta*, 2008, 75: 215–221
21 Cesarino I, Marino G, Matos JdR, Cavalheiro ETG. Evaluation of a carbon paste electrode modified with organofunctionalised SBA-15 nanostructured silica in the simultaneous determination of divalent lead, copper and mercury ions. *Talanta*, 2008, 75: 15–21
22 Jackson B, Taylor V, Baker RA, Miller E. Low-level mercury speciation in freshwaters by isotope dilution GC-ICP-MS. *Environ Sci Technol*, 2009, 43: 2463–2469
23 Liu CW, Hsieh YT, Huang CC, Lina ZH, Chang HT. Detection of mercury(II) based on Hg^{2+}–DNA complexes inducing the aggregation of gold nanoparticles. *Chem Commun*, 2008, 2242–2244
24 Xue XJ, Wang F, Liu XG. One-step, room temperature, colorimetric detection of mercury (Hg^{2+}) using DNA/nanoparticle conjugates. *J Am Chem Soc*, 2008, 130: 3244–3245
25 Darbha GK, Ray A, Ray PC. Gold nanoparticle-based miniaturized nanomaterial surface energy transfer probe for rapid and ultrasensitive detection of mercury in soil, water, and fish. *ACS Nano*, 2007, 1: 208–214
26 Huang CC, Huang YF, Cao ZH, Tan WH, Chang HT. Aptamer-modified gold nanoparticles for colorimetric determination of platelet-derived growth factors and their receptors. *Anal Chem*, 2005, 77: 5735–5741
27 Kim Y, Johnson RC, Hupp JT. Gold nanoparticle-based sensing of "spectroscopically silent" heavy metal ions. *Nano Lett*, 2001, 1: 165–167
28 Long YF, Huang CZ, Li YF. Hybridization detection of DNA by measuring organic small molecule amplified resonance light scattering signals. *J Phys Chem B*, 2007, 111: 4535–4538
29 Zhao HW, Huang CZ, Li YF. Immunoassay by detecting enhanced resonance light scattering signals of immunocomplex using a common spectrofluorometer. *Talanta*, 2006, 70: 609–614
30 Pecora R. Dynamic light scattering measurement of nanometer particles in liquids. *J Nanoparticle Res*, 2000, 2: 123–131